WARP AND WEFT DIRECTION DAMAGE DEVELOPMENT IN THE LATE-STAGE FATIGUE LIFE OF A 3D NON-CRIMP ORTHOGONAL WEAVE COMPOSITE

M.C. Poole[1], S.L. Ogin[1], P.A. Smith[1], G.M. Wells[2], P. Potluri[3], P. J. Withers[3]

[1] Faculty of Engineering and Physical Sciences, Department of Mechanical Engineering Sciences, University of Surrey, Guildford, UK
Email: m.poole@surrey.ac.uk; s.ogin@surrey.ac.uk; p.smith@surrey.ac.uk
Web page: http://www.surrey.ac.uk/mes/index.htm
[2] Platform Systems Division, DSTL, Porton Down, Salisbury, UK
Email: GMWELLS@mail.dstl.gov.uk
Web page: https://www.gov.uk/government/organisations/defence-science-and-technology-laboratory
[3]School of Materials, University of Manchester, Manchester, UK
Email: prasad.potluri@manchester.ac.uk; p.j.withers@manchester.ac.uk
Web page: http://www.materials.manchester.ac.uk/

Keywords: 3D woven composites, damage development, fatigue

Abstract

The development of damage throughout the fatigue lifetime of specimens loaded along the warp and weft directions of a three-directional non-crimp orthogonal woven (3DNCOW) composite has been studied in detail. The fundamental damage mechanisms are, not surprisingly, common to each direction (i.e. transverse cracks, interfacial debonding (Z-binder debonding, micro-delaminations) and longitudinal splits). However, the difference of fibre architecture in relation to the loading direction leads to minor differences in the details of the damage for the two loading directions. In particular, there is an increased crack density, a delay in the formation of delaminations, and a slight difference in the initiation location of Z-binder debonds, and longitudinal splits, in weft direction loaded specimens when compared to warp direction loaded specimens.

1. Introduction

Composites with through-thickness reinforcement have been an area of interest for a number of years, yet the body of work is still relatively small. These composites have been shown to improve the delamination resistance by increasing the through-thickness strength [1]; methods of achieving this include stitching [2], Z-pinning [3], or weaving 3D fabrics with dedicated through thickness Z-binders (also known as Z-tows) [4]. Many studies in the literature on 3D woven preforms have focused on quasi-static loading behaviour [5-17]. These works cover many areas including, but not limited to: mechanical properties, damage development, effect of binder paths, and failure modes. Compared to the work undertaken on quasi-static behaviour, studies relating to fatigue loading of 3D woven preforms are relatively limited [1, 18-22]. The work presented here is a development of work presented previously on the early stage damage development of 3DNCOW composites fatigue loaded in both principle (warp and weft) directions [23]. The current work provides further detailed insights into damage development as the specimens are fatigue loaded toward failure.

2. Experimental methods

In this study a 3DNCOW E-glass fabric supplied by 3TEX® has been used. It is designated “3D-78” as it has an areal density of 78oz/yd^2, or 2.64kg/m^2. The architecture of this fabric consists of three weft

Excerpt from ISBN 978-3-00-053387-7

tow layers, two warp tow layers, and Z-yarns which interlace along the warp direction (Figure 1). Of the total fibre volume content, 47.6% of fibres lie along the warp direction, 47.8% lie along the weft direction, and the remaining 4.6% lie in the z-direction. The fabric used in this study is identical in architecture and fibre to that used by other researchers [5, 6].

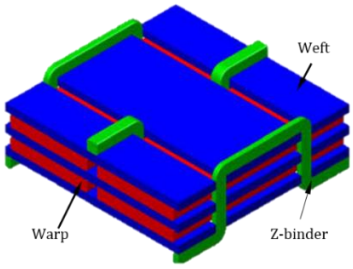

Figure 1: 3D schematic diagram of a unit cell in the 3D-78 preform [5]

Specimens were manufactured using a three part resin system and a wet impregnation technique described in [24]. The resin system consists of Epoxide Resin 300®, methyl nadic anhydride (MNA) curing agent, and the accelerator Ancamine K61B®. The combination of this resin system with E-glass fibres allows for the production of near-transparent specimens as the refractive index of the fibres and resin match closely. The fibre volume fraction content was approximately 0.47. Fatigue specimens were typically 230 mm in length. GFRP composite end tabs of length 50 mm were bonded to the ends of each specimen, leading to a specimen gauge length of 130 mm. The width and thickness of specimens were nominally 12 mm and 2.1 mm respectively. Some specimens were tested with a width of approximately 24 mm.

All tests, both quasi-static and fatigue, were performed using an Instron® servohydraulic fatigue machine with a load cell rated at 100 kN static and 50 kN dynamic. Strain was measured using an Instron® extensometer with standard gauge length of 12.5 mm and total travel of +/- 2.5 mm. The standard extensometer gauge length was used on all quasi-static tests, while an extended gauge of 96 mm was used during fatigue loading. Quasi-static tests were performed in tension and loaded at a rate of 1 mm/min until failure occurred, whereas fatigue tests were conducted under constant amplitude tension-tension conditions with a stress ratio of 0.1 and a frequency of 5 Hz.

Photographs were taken at regular cyclic intervals during each test using a high resolution camera and a backlight in order to monitor the damage developed during testing. Based on observation made using these images, specimens were sectioned in regions of particular interest; optical microscopy allowed these regions to be understood in relation to the fabric architecture.

3. Results and discussion

3.1. Quasi-static testing

In order to determine the mechanical properties of the 3DNCOW composite, quasi-static tensile tests were conducted in both principal directions. Six tests were carried out along the warp direction and eight tests along the weft. The main properties summarised in **Error! Reference source not found.**.

When comparing the warp and weft directions, it can be seen that the properties in both directions are essentially the same, though the modulus in the weft direction is slightly lower than that measured for the warp direction. These results seem reasonable since the fibre volume content is very similar in both directions. Comparing these results with those in [5], it is found that the modulus and ultimate strengths

Excerpt from ISBN 978-3-00-053387-7

reported here are higher by approximately 10% and 20% respectively. The ultimate strains on the other hand are very similar. The differences may be the result of the different resin matrix and manufacturing method (a vinyl ester resin matrix and VARTM were used in [5]).

Table 1: Mechanical properties recorded for each principal fabric direction (uncertainties quoted are standard deviations).

Loading Direction	Elastic Modulus, E (GPa)	Ultimate Strength, σ_{ult} (MPa)	Ultimate Strain, ε_{ult} (%)	Total Fibre vol. fraction, V_f
Warp	26.1 ± 0.7	519 ± 33	2.8 ± 0.2	0.47 ± 0.02
Weft	25.3 ± 0.7	514 ± 28	2.8 ± 0.3	

3.2. Late stage fatigue damage

As specimens were fatigue loaded toward failure, it was found that the level of damage developed in a specimen increases such that potential regions of failure become apparent. Previous work [23] used a low peak stress (100 MPa) when investigating the damage accumulation, for which the number of cycles to failure is greater than 10^6. To investigate damage close to failure, a higher peak stress (200 MPa) has been used in these tests, producing cycles to failure between approximately 50,000 and 200,000 cycles for loading in the warp direction and 5,000 and 30,000 for loading in the weft direction.

3.2.1. Damage development when loading in the warp direction

Figure 2 shows the damage development in a warp-direction loaded specimen from early to late stage damage development. Figure 2a highlights examples of the different damage types that form during the early stages of fatigue loading (further details can be found in Poole et al [23]. It can be seen that transverse cracking occurs in two regions during this stage: within weft tows, as matrix cracks, and along the resin channel between weft tow boundaries. The propagation of transverse matrix cracks through the thickness of the composite depends on their position; weft tow matrix cracks traversing resin pockets can grow further through the thickness, growing into other weft tow layers, via the resin pockets. It is also possible for matrix cracks to develop in other weft tow layers independently. Unlike the growth of weft tow matrix cracks, which can be slow, the growth of resin channel transverse cracks is more rapid. Most of the resin channel cracks are through-thickness, except where they intersect either the warps tows or Z-binders.

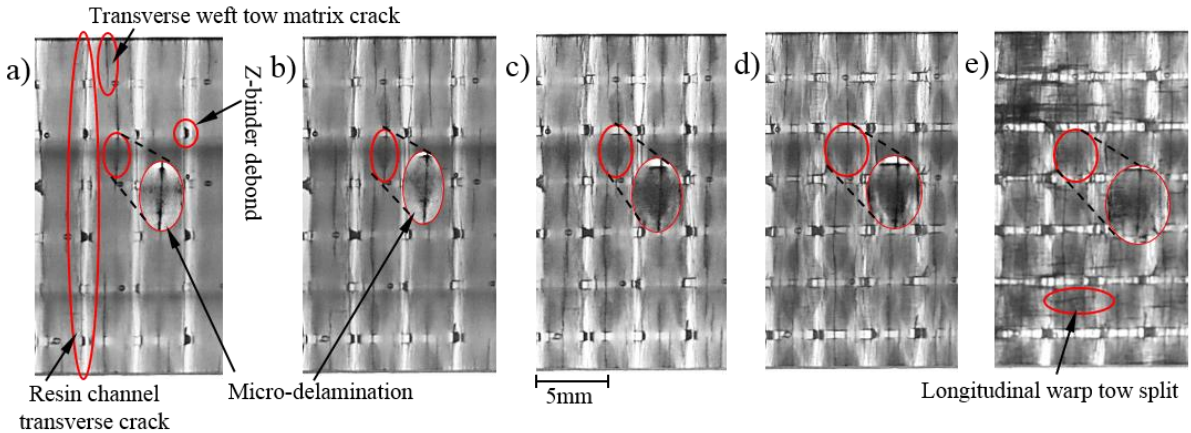

Figure 2: Plan view photographs of a specimen fatigue loaded along the warp direction with a peak stress of 200MPa; each indicating the development of damage at various stages over the specimen's fatigue life. a) 200 cycles, b) 500 cycles, c) 1,000 cycles, d) 8,000 cycles, e) 140,000 cycles

Excerpt from ISBN 978-3-00-053387-7

Other damage mechanisms indicated in Figure 2a include Z-binder debonds and micro-delaminations. Z-binder debonds are the result of interfacial debonding between the through-thickness portion of the Z-binder and surrounding material, specifically, the edge of the central weft tow layer. These debonds occur regularly throughout the material.

Micro-delaminations are tow-level interfacial fractures that occur, at least initially, at the interface between a surface weft tow and its neighbouring warp tow, and are associated with weft tow transverse cracks in the same region. Figure 2a-e follows the growth of a micro-delamination, having a curved outline, which extends across the width of a warp tow. Along one edge of the warp tow, the delamination extends towards the outer limits of the weft tow, while at the other edge of the warp tow, the delamination tends to a point; Figure 3a illustrates this growth schematically as if viewed from the surface of the specimen. In relation to the geometry of this 3D fabric, the part of the delamination tending to a point also corresponds to the crown of the Z-binder. It is as if the Z-binder is causing a pinching effect that is restricting the growth of the micro-delamination at the weft tow/warp tow interface immediately beneath the Z-crown. The architecture of the 3D fabric leads to a discernible repetition of the micro-delamination shapes (shown schematically in Figure 3b); in effect, each delamination points toward the crown of a Z-binder. Taking a cross-section close to the edge of a warp tow, although not within the Z-binder which consequently cannot be seen in this cross-section (Figure 4), it is observed that wide micro-delaminations form at the weft/warp interface furthest from the Z-crown, whilst narrower micro-delaminations form at the weft/warp interface closest to the Z-crown; this is in agreement with the schematic diagrams of Figure 3. In late stage fatigue, it has been observed that fibre fractures occur preferentially at the edge of a warp tow nearest a Z-binder crown [25]. At these locations, toward the edges of warp tows, the weft/warp micro-delaminations have reduced in width to zero, so that stress concentrations caused by weft tow transverse matrix cracks are not eliminated by the micro-delaminations here; consequently, it is not surprising to find extensive fibre fractures at these locations i.e. at the edges of warp tows.

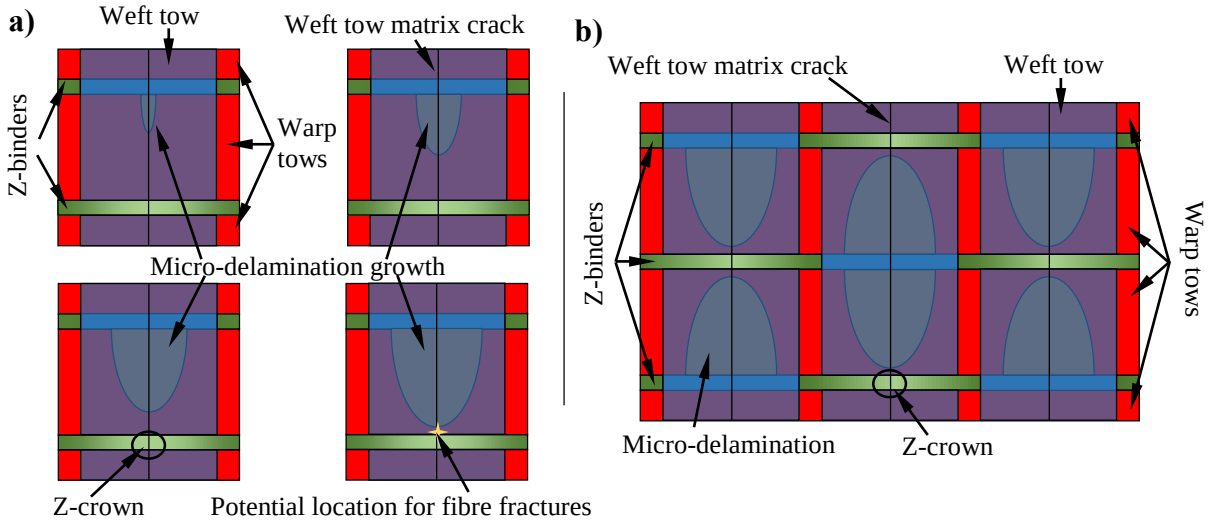

Figure 3: Diagrams indicating: a) delamination growth during fatigue loading specimens along the warp direction, b) delamination growth pattern over a larger region of the material.

The final type of significant damage which forms in warp-loaded specimens is longitudinal warp tow splitting; an example has been highlighted in Figure 2e. The splits develop within warp tows and grow at various points along the length of the specimen, extending relatively short distances. Unlike many of

Excerpt from ISBN 978-3-00-053387-7

the other damage mechanisms mentioned above, splits do not form during the early stage of fatigue loading but tend to form after transverse crack growth has saturated. Observations suggest that these splits do not contribute to the initiation of final failure in fatigue loading.

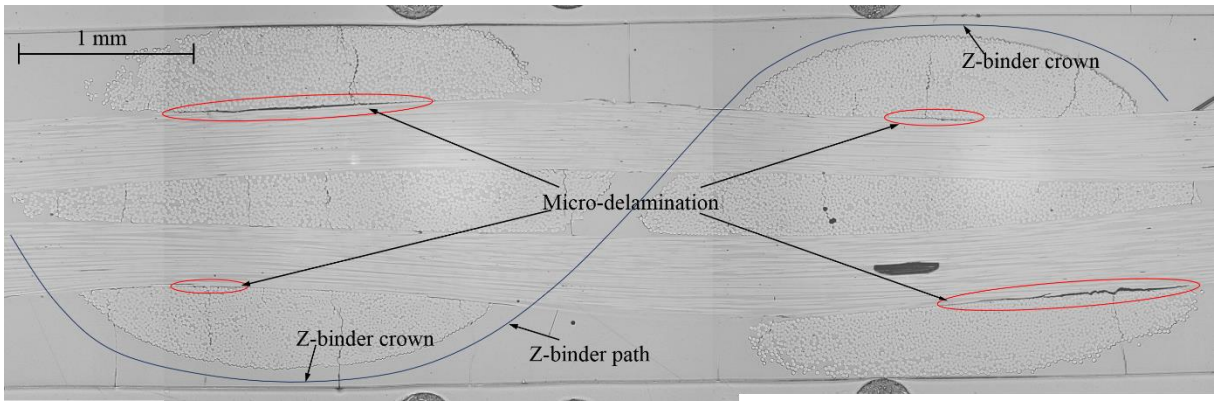

Figure 4: Micrograph cross-section of a specimen fatigue loaded with a peak stress of 200MPa showing examples of micro-delaminations

3.2.2. Damage development when loading in the weft direction

Figure 5 shows a sequence of photographs of the same area of a specimen fatigue loaded along the weft direction, indicating the extent to which damage develops over the fatigue life. In Figure 5a, examples of the main damage mechanisms that form during the early stage of the fatigue loading have been highlighted. One of the first forms of damage is transverse cracking in the warp tows. During this initial stage, warp tow transverse matrix cracks develop from each edge of the specimen. It can be seen that for each warp tow, multiple cracks form; an example of this has been circled in Figure 5a.

As loading continues (Figure 5b and c), the number of warp tow transverse matrix cracks increases, with many small cracks developing throughout the specimen. In a similar manner to warp direction loaded specimens, warp tow transverse cracks in weft direction loaded specimens can progress further through the thickness of the composite depending on their position relative to the various resin-rich regions. Compared with loading in the warp direction, the crack density (i.e. the crack area per unit volume) in weft fatigue loaded specimens is higher [26].

Other than warp tow transverse matrix cracks, transverse cracks also develop through the Z-binder and resin-rich regions adjacent to the Z-binder, as indicated in Figure 5a. These transverse cracks often extend through the entire thickness of the composite. In a similar way to the resin channel cracks observed in warp-loaded specimens, these Z-binder transverse cracks usually propagate rapidly across the specimen width and thickness.

Another damage mechanism that develops early during fatigue loading in the weft direction is Z-binder interfacial debonds; these appear, from a surface view of a transparent specimen (Figure 5a and b), as triangular-shaped damaged regions. The damage here consists of three parts: (i) an interfacial fracture between the surface weft tow and the Z-binder crown; (ii) debonding of the Z-binder from the central weft tow; and (iii), delamination between one surface of the central weft tow and the adjacent resin pocket. The combination of these three types of damage creates the appearance of two triangles, one behind the other, with the apex of both triangles facing in the same direction (Figure 5c), and the base of each triangle indicating the edge of their respective weft tow. A second pair of triangles is located at the other edge of the weft tow, with each pair facing in opposite directions (Figure 5c). As the specimen is fatigue loaded further, the Z-binder debonds continue to develop and grow, expanding to cover the entire interface between the surface weft tow and the Z-binder (Figure 5d and e).

Excerpt from ISBN 978-3-00-053387-7

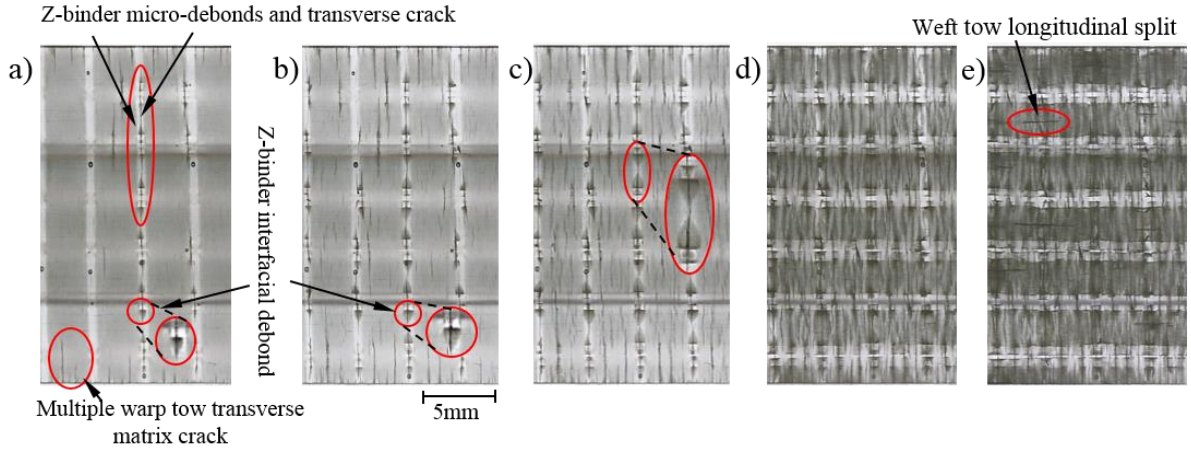

Figure 5: Plan view photographs of a specimen fatigue loaded along the weft direction with a peak stress of 200MPa; each indicating the development of damage at various stages over the specimen's fatigue life. a) 200 cycles, b) 500 cycles, c) 1,000 cycles, d) 8,000 cycles, e) 45,000 cycles

The initiation of micro-delaminations in weft-direction loaded specimens appears delayed in comparison to warp direction loaded specimens. Inspection of Figure 5a-c shows limited, if any, micro-delamination development, whilst Figure 5d has noticeable delamination growth. These micro-delaminations have formed from many of the warp tow transverse matrix cracks, and appear to extend across the width of a weft tow. Over the fatigue life of a specimen, micro-delamination growth is slow; however, as the specimen nears failure, the area covered by micro-delaminations appears quite extensive (Figure 5e).

The final damage mechanism to form during fatigue loading in the weft direction is longitudinal splitting; Figure 5e highlights an example. These splits originate from similar locations across the length of the specimen, typically from the centre of the surface weft tow and Z-binder crown; splits grow in both directions at a roughly equal rate away from the site of their initiation at the Z-binder. None of the splits were observed to grow sufficiently to link up before specimen failure. Interestingly, in contrast to final failure for the warp direction, which appears to occur through the development of fibre fractures at the edges of warp tows, for the weft direction no distinct region has been identified from which final fatigue failure develops. Indeed, it is possible that the extensive delaminations which occur throughout the weft-loaded specimens may remove the stress concentrations associated with the warp tow matrix cracks.

4. Concluding remarks

Detailed investigations of a 3D non-crimp orthogonal woven composite fatigue loaded in both principal directions (warp and weft) have revealed many differences and similarities in the damage developed. Both loading conditions have the same fundamental damage mechanisms, but in slightly different regions and forms; these include transverse cracks, interfacial debonding (Z-binder debonding, micro-delaminations) and longitudinal splits.

For specimens fatigue-loaded in the warp direction, transverse cracks developed along the weft tows and the resin channel between weft tow boundaries. Z-binder debonds are an interfacial fracture between the through thickness portion of the Z-binder and the central weft tow; these form from transverse resin channel cracks. Micro-delaminations form at the interface between the surface weft tow and the adjacent warp tow, and have a shape that points toward the nearest Z-binder crown. This narrowing of the micro-delamination near the Z-binder crown enables a stress concentration to build toward one edge of the warp tow, thus providing potential sites for warp tow fibre fractures to develop. Longitudinal splits also form at various locations along the length of the specimen within warp tows.

Excerpt from ISBN 978-3-00-053387-7

For specimens fatigue-loaded in the weft direction, transverse cracks form in both the warp tows and Z-binders. The transverse crack density appears higher in weft-loaded specimens than when loading in the warp direction. Z-binder debonds form at the interface between the surface weft tow and the Z-binder crown, and between the central weft tow and the through-thickness portion of the Z-binder; these appear, when viewed from the specimen surface, as unusual triangular-shaped damage pairs. Longitudinal splits form at the centre of the surface weft tow, directly beneath the centre of the Z-binder crown, and grow parallel to the loading direction away from the Z-binder. Micro-delaminations do not form until later in the fatigue life of weft loaded specimens compared to warp loaded specimens. However, the extent to which delaminations occur in weft loaded specimens suggests that there may be no preferential location for failure to initiate.

Acknowledgements
The authors would like to thank the EPSRC and DSTL for funding this project.

References

[1] S. Rudov-Clark and A. P. Mouritz, "Tensile fatigue properties of a 3D orthogonal woven composite," *Composites: Part A,* vol. 39, pp. 1018-1024, 2008.

[2] K. Dransfield, C. Baillie and Y. Mai, "Improving the delamination resistance of CFRP by stitching - A review," *Composites Science and Technology,* vol. 50, pp. 304-317, 1994.

[3] A. P. Mouritz, "Review of z-pinned composite laminates," *Composites: Part A,* vol. 38, pp. 2383-2397, 2007.

[4] A. E. Bogdanovich and M. H. Mohamed, "Three-Dimensional Reinforcements for Composites," *SAMPE Journal,* vol. 45, no. 6, Nov/Dec 2009.

[5] S. V. Lomov, A. E. Bogdanovich, D. S. Ivanov, D. Mungalov, M. Karahan and I. Verpoest, "A Comparative Study of Tensile Properties of Non-Crimp 3D Orthogonal Weave and Multi-layer Plain Weave E-Glass Composites. Part 1: Materials, Methods, and Principle Results," *Composites: Part A,* vol. 40, pp. 1134-1143, 2009.

[6] D. S. Ivanov, S. V. Lomov, A. E. Bogdanovich, M. Karahan and I. Verpoest, "A comparative study of tensile properties of non-crimp 3D orthogonal weave and multi-layer plain weave E-glass composites. Part 2: Comprehensive experimental results," *Composites: Part A,* vol. 40, pp. 1144-1157, 2009.

[7] L. Lee, S. Rudov-Clark, A. P. Mouritz, M. K. Bannister and I. Herszberg, "Effect of weaving damage on the tensile properties of three-dimensional woven composites," *Composite Structures,* vol. 57, pp. 405-413, 2002.

[8] B. N. Cox, M. S. Dadkhah, W. L. Morris and J. G. Flintoff, "Failure mechanisms of 3D woven composites in tension, compression, and bending," *Acta Metallurgica et Materialia,* vol. 42, no. 12, pp. 3967-3984, 1994.

[9] B. N. Cox and M. S. Dadakhah, "The macroscopic elasticity of 3D woven composites," *Journal of Composite Materials,* vol. 29, no. 6, pp. 785-819, 1995.

[10] B. N. Cox, M. S. Dadkhah and W. L. Morris, "On the tensile failure of 3D woven composites," *Composites: Part A,* vol. 27A, pp. 447-458, 1996.

[11] B. Lee, K. H. Leong and I. Herszberg, "Effect of Weaving on the Tensile Properties of Carbon Fibre Tows and Woven Composites," *Journal of Reinforced Plastics and Composites,* vol. 20, pp. 652-670, 2001.

Excerpt from ISBN 978-3-00-053387-7

[12] K. H. Leong, B. Lee, I. Herszberg and M. K. Bannister, "The effect of binder path on the tensile properties and failure of multilayer woven CFRP composites," *Composites Science and Technology,* vol. 60, pp. 149-156, 2000.

[13] J. Brandt, K. Drechsler and F. J. Arendts, "Mechanical performance of composites based on various three-dimensional woven-fibre preforms," *Composites Science and Technology,* vol. 56, pp. 381-386, 1996.

[14] J. P. Quinn, A. T. McIlhagger and R. McIlhagger, "Examination of the failure of 3D woven composites," *Composites: Part A,* vol. 39, pp. 273-283, 2008.

[15] R. Munoz, V. Martinez, F. Sket, C. Gonzalez and J. Llorca, "Mechanical behaviour and failure micromechanisms of hybrid 3D woven composites in tension," *Composites: Part A,* vol. 59, pp. 93-104, 2014.

[16] S. Vadlamani, "Damage Accumulation and Modulus Reduction During the Tensile and Flexural Loading of a 3D Woven Composite," University of Surrey, Guildford, 2010.

[17] A. E. Bogdanovich, M. Karahan, S. V. Lomov and I. Verpoest, "Quasi-static tensile behaviour and damage of carbon/epoxy composite reinforced with 3D non-crimp orthogonal woven fabric," *Mechanics of Materials,* vol. 62, pp. 14-31, 2013.

[18] V. Carvelli, G. Gramellini, S. V. Lomov, A. E. Bogdanovich, D. D. Mungalov and I. Verpoest, "Fatigue behaviour of non-crimp 3D orthogonal weave and multi-layer plain weave E-glass reinforced composites," *Composites Science and Technology,* vol. 70, pp. 2068-2076, 2010.

[19] M. Karahan, S. V. Lomov, A. E. Bogdanovich and I. Verpoest, "Fatigue tensile behaviour of carbon/epoxy composite reinforced with non-crimp 3D orthogonal woven fabric," *Composites Science and Technology,* vol. 71, pp. 1961-1972, 2011.

[20] A. P. Mouritz, "Tensile fatigue properties of 3D composites with through-thickness reinforcement," *Composite Science and Technology,* vol. 68, pp. 2503-2510, 2008.

[21] L. Yao, Q. Rong, Z. Shan and Y. Qiu, "Static and bending fatigue properties of ultra-thick 3D orthogonal woven composites," *Journal of Composite Materials,* pp. 1-9, 2012.

[22] B. Yu, R. S. Bradley, C. Soutis, P. J. Hogg and P. J. Withers, "2D and 3D imaging of fatigue failure mechanisms of 3D woven composites," *Composites: Part A,* vol. 77, pp. 37-49, 2015.

[23] M. C. Poole, S. L. Ogin, P. A. Smith, G. M. Wells, P. Potluri and P. J. Withers, "Early-stage fatigue damage development of a non-crimp 3D orthogonal weave composite loaded in the warp and weft directions," in *20th International Conference on Composite Materials*, Copenhagen, 2015.

[24] H. M. S. Belmonte, C. I. C. Manger, S. L. Ogin, P. A. Smith and R. Lewin, "Characterisation and modelling of the notched tensile fracture of woven quasi-isotropic GFRP laminates," *Composite Science and Technology,* vol. 61, no. 4, pp. 585-597, 2001.

[25] S. Topal, L. Baiocchi, A. D. Crocombe, S. L. Ogin, P. Potluri, P. J. Withers, M. Quaresimin, P. A. Smith, M. C. Poole and A. E. Bogdanovich, "Late-stage fatigue damage in a 3D orthogonal non-crimp woven composite: An experimental and numerical study," *Composites: Part A,* vol. 79, pp. 155-163, 2015.

[26] M. C. Poole, S. L. Ogin, P. A. Smith, G. M. Wells and P. Potluri, *[Paper in preparation]*, 2016.

Excerpt from ISBN 978-3-00-053387-7